

Phenomenological and spectroscopic evidence for defect-induced high-temperature superconductivity

J. C. Phillips

AT&T Bell Laboratories, Murray Hill, New Jersey 07974

(Received 13 June 1991)

Two models can provide the strong coupling required to explain high-temperature superconductivity with the established Fröhlich-Bardeen electron-phonon interaction. One utilizes quasi-two-dimensional energy bands with E_F pinned by the logarithmic saddle-point singularity in $N(E)$, while the other uses defect enhancement of $N(E_F)$. Two kinds of composition-dependent experimental data— T_c itself, and spectroscopic measurements of $N(E_F)$ and $E(\mathbf{k})$ —can be used to distinguish these models. Overall, both kinds of data favor defect enhancement.

Calculations¹⁻³ of the electron-phonon coupling constant λ for high-temperature superconductors such as $\text{YBa}_2\text{Cu}_3\text{O}_{6+x}$ have yielded values of $\lambda \lesssim 1$, whereas with reasonable phonon energies of order 0.03–0.06 eV the observed values of T_c require $\lambda \sim 3-4$. Quite early I suggested⁴ that this failure of conventional one-electron energy-band theory could be explained by a defect model with a high density of defect states $N_d(E)$ added to the usual band density of states $N_b(E)$ so that the total density of states

$$N(E_F) = N_b(E_F) + N_d(E_F) \quad (1)$$

was enhanced by a factor of 3 or 4 over a typical band value. The defects may be oxygen vacancies of interstitials or antisite cations, whose nature is not discussed further here. A second approach⁵⁻⁷ assumes that the bands are more nearly two-dimensional (2D) than appears in one-electron calculations¹⁻³ (for example, because of self-trapping of single-particle states in layers due to strong electron-phonon interactions). Then one can obtain a strong peak in $N(E)$ of the form

$$N(E) \sim \ln|E_F/(E - E_F)| \quad (2)$$

due to critical saddle points, which may also increase λ and T_c enough to agree with experiment. In both cases the composition and processing required to maximize $N(E_F)$ are determined empirically. In the defect model⁴ the pinning is further favored by the large and empirically highly variable polarizability and diffusivity of oxygen anions.

It may seem, at first, as if these two mechanisms, both of which involve enhancement of $N(E_F)$, are so similar as to be experimentally indistinguishable. The purpose of this paper is to examine two kinds of evidence which might be used to separate the two mechanisms. The first, which I believe is more revealing, is phenomenological and relates $N_d(E_F)$ to lattice instabilities and to the composition dependence of T_c . The second kind of evidence is spectroscopic, but it seems unlikely to be able to resolve $N_b(E_F)$ and $N_d(E_F)$ because the intrinsic structure in $N(E_F)$ is masked by an incidental but very large background generated by the high energy of the probe particles (photons or electrons).

When Fröhlich first proposed⁸ that electron-phonon in-

teractions could be attractive and lead to superconductivity, he remarked that increasing the electron-phonon coupling would not only increase T_c but would also eventually produce lattice instabilities. If we consider some variable X (which could be the electron/atom ratio, or the lattice constant, or some internal coordinate of the unit cell), we can define X so that for small X we have $dT_c/dX > 0$. Then there are three possibilities (I–III) for the relative positions of the values of X which maximize $T_c(X_m)$ and which produce a lattice instability (X_{li}). These are illustrated in Fig. 1 and the upper panel of Fig. 2. In type I we have T_c increasing monotonically up to $X = X_{li}$, so that $X_m = X_{li}$. This is the case for Tl–Pb–Bi alloys.⁹ In type II, T_c increases, peaks, and decreases and eventually a phase transition occurs for larger X which is unrelated to $N(E_F)$. In this case λ and T_c do not become large enough to cause a first-order phase transition, but there may be evidence for lattice relaxation at the maximum T_c , as in NbN and ZrN and related compounds.¹⁰

A third type of behavior (III) has been found for high-temperature oxide superconductors, which include not only $\text{YBa}_2\text{Cu}_3\text{O}_{6+x}$, $\text{Bi}_2\text{Sr}_2\text{CaCu}_2\text{O}_{8+y}$, and $\text{Tl}_2\text{Ba}_2\text{CuO}_{6+y}$, which are layered, but also $\text{Ba}_{1-x}\text{K}_x\text{BiO}_3$, which is cubic. In these cases with increasing X we have T_c increasing to a maximum at $X_m = X_{li}$ where $dT_c/dX = 0$. For larger X either the compound cannot be formed¹¹ ($\text{YBa}_2\text{Cu}_3\text{O}_{6+x}$ with $X \gtrsim 1$), or it phase separates¹² ($\text{Bi}_2\text{Sr}_2\text{CaCu}_2\text{O}_{8+y}$ and $\text{Tl}_2\text{Ba}_2\text{CuO}_{6+y}$, with $y = 1 - X < 0.1$), or it becomes insulating with only¹³ minor structural changes ($\text{Ba}_{1-x}\text{K}_x\text{BiO}_3$ with $x = 1 - X < 0.37$). All of these results are readily explained by defect pinning of E_F , but not by the saddle-point model, as we shall now see.

The distinguishing feature of the two models shown in Fig. 1 is that in the defect-enhancement model (lower panel) the defects have a narrow ($\lesssim 0.1$ eV) band which pins E_F , whereas in the 2D saddle-point model (upper panel) the defect bands are at energies E_r with $|E_r - E_F| \gtrsim 1$ eV. In that case increasing the defect density with increasing X merely reduces the strength of the band states and broadens them with increasing $|E - E_F|$. This means that the saddle-point model predicts type II behavior. The difference in the two models becomes apparent when the defect concentration is so large that

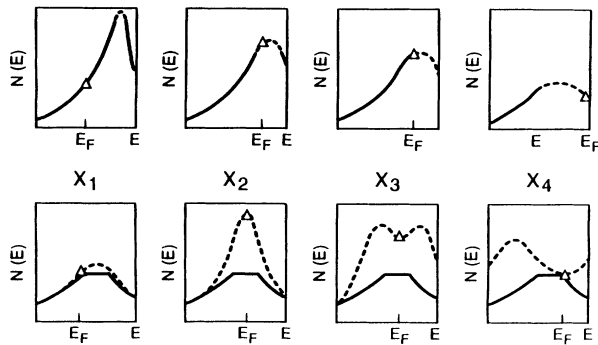


FIG. 1. Sketches of the behavior of the density of states $N(E)$ as a function of composition X in a high- T_c alloy series, with X_j increasing with increasing j ($=1-4$). As X increases, E_F moves towards the peak in $N_b(E)$ and the defect density increases. This movement of E_F includes the effects of interlayer charge transfer as well as charge addition, but the concomitant defect-density variations are neglected in conventional Fermi-liquid models. Upper panel: 2D band peak in $N(E)$ cutoff (dashed line) by defect broadening, the latter increasing as X increases. Lower panel: the defect-enhancement model. The defect states introduce an N_d band centered at or within 0.1 eV of E_F , which also contains a peak in N_b associated with 3D band states; the width of this peak is about 0.1 eV. In both models the peak in $N(E)$ and T_c occurs near $X=X_2$. In the defect-enhancement model, however, for larger $X \gtrsim X_3$ the defect contribution (indicated by the difference between the dashed and solid lines in the lower panel) splits into "bonding" ("antibonding") bands below (above) E_F which herald the onset of lattice instability. In each figure $N(E_F)$ is marked with a triangle to make it easier to follow $N(E_F)$ as a function of X .

defect-defect interactions become important for $X \gtrsim X_3$. This has little effect on the saddle-point model, where T_c peaks near $X=X_2$, because this is the value of X at which E_F reaches the edge of the cutoff 2D peak in $N(E)$. In other words, because there is no defect band at E_F , the lattice instability will arise in connection with the defect bands at E_F and for values of X well removed from X_2 .

The situation is different for the defect-enhancement model (lower panel of Fig. 1). Now when the defect band begins to split due to defect-defect interactions, this causes $N(E_F)$, which is dominated by $N_d(E_F)$, to decrease. Thus, X_m and X_{li} should be nearly equal in the defect-enhancement model. Moreover, as X approaches $X_m \approx X_{li}$ in this model, dT_c/dX tends toward zero because $N_d(E_F)$ is becoming a broad, flat peak with

$$d^n N/dE_F^n \rightarrow 0, \quad n=1-3. \quad (3)$$

However, if the defects are mobile the defect-enhancement model predicts type III behavior. If the lattice instability arises from short-range forces and rearrangement of electronic states well removed from E_F , then we have case I. This is the situation in Pb-Bi alloys, where the metallic structure of Pb is replaced by the essentially covalent structure of Bi due to the latter's formation of short (sp^2) and long (s^2p^3d) bonds.

We now turn to the lower panel of Fig. 2, which con-

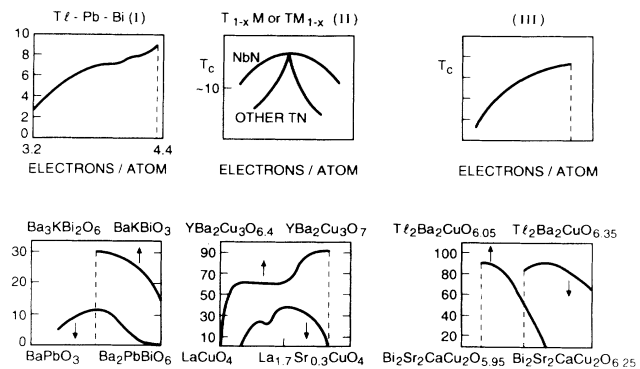


FIG. 2. The three types (I-III) of composition dependence of T_c (upper panel). In type I (upper left) there is no special behavior of $N(E_F)$ and the monotonic increase of E_F is interrupted by a first-order phase transition associated with short-range forces. In type II a peak in T_c is associated with a peak in $N(E_F)$, as in $T_{1-x}M_{1-y}$ alloys, where T is a transition metal and M is a metalloid (such as C, N, or O). In type III behavior $dT_c/dX=0$ at $X=X_i$. In the lower panel experimental data for several high-temperature superconductors are shown for comparison with the upper panel.

tains high- T_c examples of type III behavior, including $YBa_2Cu_3O_{6+x}$, $X_m=X_{li}=0.9$; $Bi_2Sr_2CaCu_2O_{9-x}$, $X_{li}=X_m=0.85$ (the T_c 's at $X=0.90$ and 0.85 are probably different because of the presence of a second phase); $Tl_2Ba_2CuO_{7-x}$, $X_m=X_{li}=0.90$; and $Ba_xK_{1-x}BiO_3$, $X_{li}=X_m=0.63$. From this figure it seems that $X_m \neq X_{li}$ in $BaPb_{1-x}Bi_xO_3$ and $La_{2-x}Sr_xCuO_4$, so that these materials may be describable by band theory without defect enhancement of $N(E_F)$ and T_c . Before one accepts this conclusion, one should note that the condition $X_{li}=X_m$ in the defect-enhancement model assumes that the defects are sufficiently mobile that defect-defect bond formation can lead to phase instability. This is certainly the case for oxygen defects in cuprates, and monovalent K^+ should be mobile in $(Ba,K)BiO_3$. However, tetravalent Pb^{4+} is presumably much less mobile than K^+ . Similarly in $(La,Sr)_2CuO_4$ it is believed¹⁴ that a dominant defect is the neutral complex Sr_2O^\square , where O^\square is an oxygen vacancy shared by two Sr which are nearest neighbors on the La sublattice, and this complex may be quite immobile. This reasoning can also explain the difference between $T_c(X)$ for NbN and for other TN compounds in the upper center panel of Fig. 2. The TN compounds ($T \neq Nb$) are not defect enhanced and T_c degrades rapidly away from its peak. On the other hand, NbN is defect enhanced, and the flat $T_c(X)$ is explained by Eq. (3) with immobile defects.

The mobile defect-enhancement model also explains¹⁵ why dT_c/dP and the oxygen isotope shift dT_c/dm_0 are so small in type III cuprates. Both the pressure P and the oxygen content x_0 are examples of the generalized coordinate X , and the optimal oxygen content itself is dependent on the isotope mass m_0 . This explains why dT_c/dP and dT_c/dm_0 are both small^{16,17} in $YBa_2Cu_3O_{6.9}$ and the (2:2:1:2) Bi and Tl compounds; in all cases $dT_c/dX \rightarrow 0$ because E_F is pinned by a peak in $N(E)$ when $X=X_m$. In

(Y,Pr)Ba₂Cu₃O_{6.9} alloys the strength of an "extra" vibrational band associated with defects grows rapidly with increasing T_c and decreasing oxygen isotope shift.¹⁸

Can the differences in electronic structure near E_F of the saddle-point and defect-enhancement models be detected optically? The existence of quasiparticle states in good agreement with band-structure calculations has been established by angle-resolved photoemission.^{19–21} However, the angle-dependent peaks associated with the band states are superimposed on a large background due to phonon-assisted indirect transitions. In the photoemission experiments it is difficult to separate the peaks from the background, but in recent angle-resolved inverse photoemission experiments²² the separation is easy and it is apparent that the strength of the integrated background is about 10^2 times that of the quasiparticle peaks. This means that the defect contribution $N_d(E)$ for E near E_F is largely masked by the background. To overcome this problem photoemission, x-ray²³ and inverse photoemission²² data have been analyzed in Bi₂Sr₂Ca_{1-x}Y_xCu₂O_{8+y} alloys which are both superconductive ($x=0$) and insulating ($x \geq 0.4$). The results show a band structure which does not shift (on a scale of $\lesssim 0.2$ eV) with alloying, together with a peak at E_F which decreases with x , and thus is assigned to an "impurity state" which combines with band states to form a "Fermi-liquid state." To the extent that these samples are not phase separated (which is difficult to prove on a scale $\lesssim 50$ Å) this is evidence for defect enhancement of $N(E_F)$ and T_c . The hybrid impurity-band state raises localization questions which are discussed elsewhere.²⁴

The central weakness of the defect model is that it assumes that E_r accidentally equals E_F in a CuO_x environment. Earlier I argued²⁵ that this accident was plausible in the context of the Mattheiss relation $E(\text{Cu } 3d) = E(02p)$ for the tight-binding parameters which fit the energy bands of the ideal crystal. Much more direct and plausible is the evidence²⁶ for the anomalous dependence of dT_c/dP and dT_c/dx in the cubic chalcogenide ($C=S, \text{Se, or Te}$) $M_Y\text{Mo}_6\text{C}_{8-2}\text{O}_X$ Chevrel compounds for $M=\text{Cu}$ compared to $M=\text{Sn, Pb, or Eu}$. In all cases for the same volume change $\Delta T_{c,x} \sim 10\Delta T_{c,P}$, indicating the inadequacy of a rigid-band model. Moreover, in all cases except $M=\text{Cu}$, dT_c/dx and $dT_c/dP < 0$, but for Cu alone

the sign is reversed. In the defect model this is immediately explained by $E_r \neq E_F$ in all cases except Cu, but for CuO_xC_{2-x} complexes (where C[□] is a chalcogenide vacancy) $E_r = E_F$ to within the level width (about 0.1 eV). Thus this result shows that CuO_x complexes produce a defect state which pins E_F even in a chalcogenide medium. The pinning is a general property of the complex and is nearly independent of the distant structure of the environment, although the enhancement of T_c can be much larger for the oxide environment which can accommodate a 10^2 larger defect density without phase separation.²⁷

In conclusion, the phenomenology associated with lattice instabilities not only provides evidence for giant defect-enhanced electron-phonon interactions as the mechanism responsible for high- T_c superconductivity,⁴ but it also enables us to analyze the effects of defect mobility and sample inhomogeneities which can cause confusion in the context of even the most sophisticated spectroscopic experiments. Ultimately we expect that exploration of defect systematics^{28,29} will probably provide the most complete picture of the electronic structure and giant electron-photon interactions in high- T_c superconductors. However, the present model already enables us to understand not only the data discussed here but also to explain³⁰ why the maximum T_c obtainable in compounds formed of alternating metallic and semiconductive layers is so much higher than in fully metallic three-dimensional compounds such as Nb₃Sn.

Note added. After this paper was completed several important additional points which enable us to distinguish between smooth composition dependence of T_c [as in Ba(Pb,Bi)O₃ and (La,Sr)₂CuO₄] and discontinuous (type III) behavior became known. First, Cava *et al.* have shown²⁷ that (La,Sr)₂CaCu₂O_{6+δ} is a type III material, which helps to explain why its T_c^{max} is 20 K higher than that of (La,Sr)₂CuO₄, at nearly identical doping levels. Note that all type III materials contain either Y or Ca ionic (no oxygen) planes. Second, Motida has noted³¹ a strong correlation between T_c^{max} and the M-O bond lengths ($M=Y$ or Ca) in all type III materials. This is consistent with the dominant T_c -enhancing defect being associated with the ionic Y or Ca planes which are absent in the smooth composition dependence, medium T_c materials.

¹W. Weber, Phys. Rev. Lett. **58**, 1371 (1987); W. Weber and L. F. Mattheiss, Phys. Rev. B **37**, 599 (1988).

²P. B. Allen, W. E. Pickett, and H. Krakauer, Phys. Rev. B **36**, 3926 (1987); **37**, 7482 (1988).

³R. L. Cohen, W. E. Pickett, and H. Krakauer, Phys. Rev. Lett. **64**, 2575 (1990); C. Thomsen *et al.*, Solid State Commun. **75**, 219 (1990).

⁴J. C. Phillips, Phys. Rev. Lett. **59**, 1856 (1987).

⁵J. E. Dzyaloshinski, Pis'ma Zh. Eksp. Teor. Fiz. **46**, 97 (1987) [JETP Lett. **46**, 118 (1987)]. This paper mentions alternatives to Cooper pair formation: either charge-density or spin-density wave instabilities. To my knowledge there is no experimental evidence which would indicate any relation between the major lattice instabilities discussed here and these minor

electronic instabilities.

⁶J. Friedel, J. Phys. Condens. Matter **1**, 7757 (1989).

⁷C. C. Tseui, D. M. Newns, C. C. Chi, and P. C. Pattnaik, Phys. Rev. Lett. **65**, 2724 (1990).

⁸H. Fröhlich, Phys. Rev. **79**, 845 (1950); G. Wentzel, *ibid.* **83**, 168 (1951); H. Fröhlich, Proc. R. Soc. London, Ser. A **215**, 291 (1952).

⁹R. C. Dynes and J. M. Rowell, Phys. Rev. B **11**, 1884 (1975).

¹⁰J. K. Hulm and R. D. Blaugher, in *Superconductivity in D- and F-Band Metals*, edited by D. H. Douglass, AIP Conf. Proc. No. 4 (AIP, New York, 1971), p. 1; L. R. Testardi, Rev. Mod. Phys. **47**, 637 (1975); J. C. Phillips, Phys. Rev. Lett. **26**, 543 (1971); *Physics of High- T_c Superconductors* (Academic, San Diego, 1989), pp. 2, 31, 42, 70, 78, 81, 172, 174, 201,

- 221, 298, 326.
- ¹¹R. J. Cava *et al.*, Phys. Rev. B **26**, 5717 (1987).
- ¹²Y. Shimakawa, Y. Kubo, T. Manako, and H. Igarashi, Phys. Rev. B **40**, 11 400 (1989); C. Allgeier and J. S. Schilling, Physica C **168**, 499 (1990).
- ¹³S. Pei *et al.*, Phys. Rev. B **41**, 4126 (1990); L. F. Mattheiss (private communication) notes that near the metal-insulating boundary the structural distortions reported by Pei *et al.* are too small to produce insulating behavior as in BaBiO₃ [L. F. Mattheiss and D. R. Hamann, Phys. Rev. B **28**, 4227 (1983)]. This difficulty can be resolved with insulating domain walls not detected by diffraction, for example; see J. C. Phillips and K. M. Rabe, Phys. Rev. Lett. **66**, 923 (1991).
- ¹⁴L. C. Smedskjaer *et al.*, Phys. Rev. B **36**, 3903 (1987).
- ¹⁵J. C. Phillips, Phys. Rev. B **36**, 861 (1987).
- ¹⁶B. Batlogg *et al.*, Phys. Rev. Lett. **59**, 912 (1987); T. A. Falten *et al.*, *ibid.* **59**, 915 (1987).
- ¹⁷S. Klotz, J. S. Schilling, and W. Reith, Bull. Am. Phys. Soc. **36** (3), A24 2 (1991); S. W. Tozer, *ibid.* **36** (3), A24 3 (1991); N. E. Moulton, E. F. Skelton, and S. Wolf, *ibid.* **36** (3), A24 1 (1991); I. V. Berman *et al.*, Pis'ma Zh. Eksp. Teor. Fiz. **47**, 634 (1988) [JETP Lett. **47**, 733 (1988)]; H. Katayama-Yosida *et al.*, Physica C **156**, 481 (1988).
- ¹⁸J. C. Phillips, Phys. Rev. Lett. **64**, 1605 (1990).
- ¹⁹T. Takahashi *et al.*, Phys. Rev. B **39**, 6636 (1989).
- ²⁰J.-M. Imer *et al.*, Phys. Rev. Lett. **62**, 336 (1989).
- ²¹C. G. Olson *et al.*, Phys. Rev. B **42**, 381 (1990).
- ²²T. Watanabe *et al.*, Physica C **176**, 274 (1991).
- ²³H. Matsuyama *et al.*, Physica C **160**, 567 (1989).
- ²⁴J. C. Phillips, Phys. Rev. B **42**, 8623 (1990).
- ²⁵J. C. Phillips, *Physics of High-T_c Superconductors* (Ref. 10), p. 148.
- ²⁶D. W. Capone, R. P. Guertin, S. Foner, D. G. Hinks, and H. C. Li, Phys. Rev. B **29**, 6375 (1984); W. H. Wright *et al.*, J. Low Temp. Phys. **68**, 109 (1987).
- ²⁷Not only do the Chevrel data exclude a two-dimensional Van Hove peak as the origin of high T_c , but together with $T_c = 60$ K in La_{1.6}Sr_{0.4}CaCu₂O₆ [R. Cava *et al.*, Nature (London) **345**, 602 (1990); and (private communication)] they argue strongly against "magic" charge concentrations for a rigid-band model.
- ²⁸Z. Tan *et al.*, Phys. Rev. Lett. **64**, 2715 (1990).
- ²⁹J. C. Phillips, Phys. Rev. B **42**, 6795 (1990).
- ³⁰J. C. Phillips, Phys. Rev. B **40**, 8774 (1989).
- ³¹K. Motida, J. Phys. Soc. Jpn. **60**, 3194 (1991).